APPLICATION OF NASTRAN TO PROPELLER-INDUCED SHIP VIBRATION

By Atis A. Liepins
Littleton Research and Engineering Corp.

John H. Conaway
Control Data Corporation

SUMMARY

An application of the NASTRAN program to the analysis of propeller-induced ship vibration is presented. Described are the essentials of the model, the computational procedure, and experience. Desirable program enhancements are suggested.

INTRODUCTION

The propeller, operating in the uneven wake of a ship, generates harmonic forces which are transmitted to the hull partly through the shaft and partly through the water as hull surface pressures. The frequency of the propeller forces is determined by the number of blades on the propeller and the revolving speed of the shaft. For modern commercial ships this frequency is, at full power, in the range of 5 to 15 Hz. The fundamental frequency of these ships is of the order of 1 Hz or lower. Thus, the propeller excitation is of high frequency relative to the fundamental of the ship. The response of the ship to this excitation can be expected to be found primarily in complicated modes that are far above the fundamental.

The concern about propeller-induced vibration is seldom for its effect on the ship's structural integrity or fatigue, but rather for its effect on the habitability of crew quarters and the excessive wear of propulsion machinery. The prediction of vibration levels is thus of considerable importance in ship design, but it has been and continues to be a difficult problem. Vibration levels have been predicted from models which idealize the ship as a system of beams (Ref. 1 and 2). Although these models can handle the beam-type vibrations of the hull and the propulsion shaft, the finite-element method is more suitable when the vibration of more localized structures such as the machinery space, shaft bearing supports, and superstructures are also to be predicted (Ref. 3). Because of interest in relatively high frequency response the finite element models tend to be large. NASTRAN was selected for this problem because of its ability to handle large models. The MacNeal-Schwendler NASTRAN available at Control Data Corporation Data Centers was used. At the time that the computations were performed, Version 13 was current.

MODEL

The model is expected to represent the major types of ship vibration modes. These include the hull vertical bending, lateral bending coupled with torsion, and longitudinal extension (accordion type); the shaft longitudinal, vertical and lateral modes; the vertical motion of the double bottom and its interaction with the shaft longitudinal modes; and the motions of the superstructure. The torsional modes of the propulsion shafting and machinery are of little importance to hull vibration and are not included in the model. The local motions of the decks and shell panels are also excluded. In the operating frequency range there are typically a dozen vertical, four or five lateral-torsional, one or two longitudinal hull modes and several shafting modes.

The structure and weight distribution of the ship are nearly symmetrical about the longitudinal center plane. The minor asymmetries that exist were ignored and only one-half of the ship (the port side) was modeled.

Approximately, the forward third of the ship was modeled as a beam (fig. 1). This gross simplification of the structure is justified because it is far removed from the excitation and generally experiences low levels of vibration. The remaining structure was represented in three dimensions (figs. 2 and 3). In the three dimensional part the vertical spacing of the grid points was determined largely by the decks and the double bottom. The lateral spacing was determined by the location of longitudinal girders and bulkheads, and the attempt to limit the aspect ratio of triangular and quadrilateral elements to 2.0. The longitudinal spacing varies. Below the second deck and aft of FR 106, the longitudinal grid spacing is the finest. At shaft support structures each frame was represented. Away from these structures two or three frames were lumped. In the engine room the longitudinal spacing was also determined in part by the depth of the double bottom. Above the second deck and forward of the engine room, the grid spacing was determined by the location of major transverse bulkheads and the expected wave length of vertical vibration at a frequency corresponding to 150% of full power RPM. This resulted in the lumping of four to six frames.

The center shaft is raked and the wing shafts are raked and splayed. For these reasons the grid points of each shaft were referred to a special coordinate system. Grid points were also assigned to the centers of gravity of major machinery items such as boilers, condensers, turbines, and reduction gears.

The shell plate, double bottom, decks, bulkheads, transverse diaphragms (floor) and major machinery foundations were modeled with triangular and quadrilateral membrane elements CTRMEM and CQDMEM1. The CQDMEM1 element was selected because of its linear strain gradient (Ref. 4). Membrane elements rather than plate bending elements were used since, in vibration, the principal action of these structures is in their plane with negligible bending.

Shafts, longitudinal girders, frames, and columns were modeled with CBAR elements. Stiffeners and flanges of machinery foundations were represented by CONRODs. Shaft bearings were represented with rigid elements RBE1 and spring elements CELAS2.

The mass of the ship for vibration purposes consists of the structure, machinery, outfit, liquids in tanks, stores, cargo, and the added mass of water associated with vibration in the vertical and horizontal directions. In the forward part of the ship, represented by beam elements, mass moments of inertia, as well as masses were assigned to grid points. This was accomplished with CONM1 elements. CONM2 elements were used for machinery items, outfit, liquids in tanks, and stores. CMASS2 elements were used for the added mass of water. The structure weight generator together with an adjusted material density was used to compute the structural weight.

Multipoint constraints were used to connect the beam part of the ship hull model to the three-dimensional part, to connect the centers of gravity of major machinery items to the ship's structure, and to transfer moment from a beam element into the plane of a membrane element. MPCs were also used to interpolate displacements at grid points which, if connected by membrane elements, would result in too large aspect ratios or, if not connected, would result in gaps between membrane elements.

Single point constraints were used to eliminate singular displacement coordinates and to specify symmetry and antisymmetry conditions on the center plane.

The model consisted of 1657 grid points connected by 5667 elements, approximately evenly divided among CBAR, CONROD, CTRMEM and CQDMEM1 elements. The coordinates and constraints of the symmetric and antisymmetric models are summarized below:

	Symmetric	Antisymmetric
Multipoint constraints	332	328
Single point constraints	4,104	4,254
Unconstrained degrees of freedom	5,506	5,360
Dynamic degrees of freedom	258	228

COMPUTATIONAL PROCEDURE

For debugging purposes the model was divided into three sections: forebody, superstructure, and engine room. The forebody extends forward of FR 106, the superstructure aft of FR 106 and above the second deck, and the engine room aft of FR 106 and below the second deck (See fig. 1). Since there is interest in the modes of the engine room section when it is supported at its periphery, this division is logical.

The debugging of each section proceeded as follows using Rigid Format 3:

1) Data errors were corrected and a half a dozen undeformed geometry plots were made. The plots were examined and, if necessary, the geometry and connectivity corrected.

2) The BANDIT (ref. 5) program was used to resequence grid points.

3) The stiffness and mass matrices were assembled. The total mass in each of three directions was computed and the GPSP table, corresponding to the case of no single point constraints, was printed. This run was checkpointed and execution stopped after the GPSP table.

4) The structural weight as computed by the structural weight generator was brought into agreement with the section weight information by adjusting the density of the material. The singularities in the GPSP table were examined and for each singularity a single point constraint coded. The problem was restarted and mode shapes were computed. For the first few modes the forces of single point constraint were also computed.

5) Modes were examined for "soft spots", that is, coordinates with low stiffness and/or large mass concentration. The frequencies of some modes were checked against hand calculations, preliminary computer calculations, and general experience. If necessary, stiffness and/or mass connectivity was changed to improve the model. The single point constraint forces were inspected for their reasonableness.

Next the three sections were merged and the debugging steps 1-4, used for each section, were repeated. The BANDIT run for the merged model resulted in a bandwidth too large for NASTRAN. Apparently, this was caused by the large number of multipoint constraints. Since the multipoint constraints generally involved coordinates at three grid points, a dummy triangular membrane element CTRMEM was coded for each multipoint constraint. BANDIT then produced a resequence, which resulted in 294 active columns and a bandwidth of 19. The dummy CTRMEMs were not used in NASTRAN runs.

To insure that the more than 4000 single point constraints would suppress all singular coordinates but not destroy rigid body modes, the model was subjected to static enforced displacements. This was done through the SPCD cards. The same coordinates which later in modal extraction were specified on the SUPORT card were forced to displace so as to produce rigid body motions of the model. This calculation was first performed on the symmetric model by using Rigid Format 1.

After the symmetric model had passed the enforced rigid-body displacement check, the problem was restarted in Rigid Format 3 and 68 mode shapes were computed in the frequency range 0 to 20 Hz. For each mode shape five plots were produced:

1) An elevation view at the center plane of the engine room and superstructure,

2) An elevation view of the center plane of the forebody,

3) An elevation view of the center shaft,

4) Elevation and plan form views of the wing shaft.

Representative mode shape plots are shown in figures 4, 5, 6 and 7.

Largely as a result of the thorough checking of the three sections and the enforced rigid-body displacement check of the merged model, the modal extraction run was immediately successful.

The problem was then restarted into Rigid Format 1 and the antisymmetric enforced rigid body displacements were calculated. This was necessary since the symmetric and antisymmetric multipoint constraint sets were different, and resulted in different grid point singularity tables, and therefore different single point constraints. Subsequent to this check, the antisymmetric model was restarted into Rigid Format 3 and 64 mode shapes in the frequency range 0 - 20 Hz were computed. Since antisymmetric modes are difficult to plot, only one plot, a fore and aft view at FR 106, was produced for each mode shape.

The running times, in ARUs (Application Resource Units, a billing unit for the CDC 6600 computer) for the symmetric and antisymmetric mode extraction runs were as follows:

	Input/ Output ARUs	Central Processor ARUs	Total ARUs
Symmetric model	11,690	18,518	26,674
Antisymmetric model	8,366	14,187	19,959

The ARUs for the major modules in the case of the symmetric model were as follows:

	Input/ Output ARUs	Central Processor ARUs
SMA1	418	975
MCE2	147	888
SMP1	4,925	9,328
SMP2	1,959	3,975
READ	197	832
SDR1	824	1,428

The above table indicates that the most time-consuming operation is the condensation of stiffness and mass matrices.

Response to harmonic propeller excitation was calculated at 65 frequencies in the frequency range of 0 -20 Hz. This was done by restarting the checkpointed mode shape runs of Rigid Format 3 into Rigid Format 11.

Rigid Format 11 was altered with RF11/15 (Ref. 6) to suppress the calculation of single point constraint forces. All computed modes were used in the superposition and the same damping value was used for all modes. Responses for the following loadings were calculated:

1) The response of the symmetric model to the symmetric load components of the center propeller.

2) The response of the symmetric model to all load components of the wing propeller.

3) The response of the antisymmetric model to the antisymmetric load component of the center propeller.

4) The response of the antisymmetric model to all load components of the wing propeller.

In each of the above four cases, displacements were calculated and plotted at the propellers and several locations on the shafts, major machinery items, the bridge deck, and in the crew quarters. This resulted in 45 symmetric and 23 antisymmetric response curves. A typical response plot of displacement and phase is shown in figure 8.

The response calculation times for each of the four loading cases were 5536, 5458, 5006 and 4796 ARUs. Approximately 55 percent of the above ARUs were spent in recovering the dependent components of displacements.

CONCLUSIONS AND DESIRED ENHANCEMENTS

NASTRAN was successfully applied to the problem of propeller-induced ship vibration. All goals set at the beginning of the analysis were accomplished except those associated with damping. It was intended that the model dissipate energy through structural damping and viscous dashpots. These, however, could not be handled in an economic way, within the computational procedure described above, with Rigid Format 11 and the published RF ALTERS (Ref. 6).

NASTRAN's ability to handle the model without substructuring was especially advantageous. The aversion to substructuring resulted from experience with a previous ship vibration analysis, in which the logistics of the substructuring process were found to be time consuming. However, use of the new MacNeal-Schwendler NASTRAN superelement capability, which simplifies the substructuring process considerably, should receive consideration in future ship vibration analyses.

As a result of this computational experience, the following program enhancements are suggested:

1) Coding a large number of single point constraints to eliminate singular displacement coordinates for a three-dimensional model with complex geometry and connectivity is a time-consuming and error-prone process. An option to instruct NASTRAN to remove all singular coordinates would be desirable. This need not result in blind trust in the program if all singularities removed by the program are printed.

2) The singularities in the GPSP table can be unreliable when displacement coordinates and grid point geometry are referred to a special coordinate system. This deficiency should be corrected.

3) An automatic grid resequencing option within NASTRAN would be desirable. This option would streamline the computational process.

4) Rigid Format 11 automatically recovers the dependent coordinate displacement responses. In the present analysis there was no interest in the responses of the dependent coordinates, but more computer time was spent in their recovery than in computing the response of the independent coordinates. It is suggested that an option be included in Rigid Format 11 to avoid this computation.

5) Upon restarting, changes in mass connectivity and material density on the MAT1 card result in the recomputation of the unconstrained stiffness matrix KGGX. In this analysis a considerable amount of computer time could have been saved if mass changes did not cause the recomputation of the stiffness matrix.

6) It would be desirable to have structural damping (i. e., proportional to displacement and independent of frequency) in Rigid Format 11. Although the User's Manual (Ref. 7) describes the TABDMP1 card as

"Structural Damping", it is used as viscous modal damping as indicated by the equations in Section 3.12.2 of the User's Manual. The published ALTER RF 11/4 (Ref. 6) inserts structural damping into Rigid Format 11. This ALTER worked successfully when tested in a cold start sample problem, but failed in the computational procedure described in the preceding section.

Many restart failures were experienced during this analysis. Some failures were due to acknowledged program errors. Others resulted from the use of multiple restarts in conjunction with published Rigid Format ALTERS. These restart failures demonstrated that in order for the structural dynamicist to compute effectively with NASTRAN, access to an analyst, knowledgeable in NASTRAN restart logic, is essential.

REFERENCES

1. McGoldrick, R. T., "Ship Vibration", David Taylor Model Basin Report 1451, December 1960.

2. Reed, F. E., "The Design of Ships to Avoid Propeller-Excited Vibration" SNAME, Vol. 79, 1971, pp. 244-296.

3. Restad, K., et al, "Investigation of Free and Forced Vibrations of an LNG Tanker with Overlapping Propeller Arrangement" SNAME, Vol. 81, 1973, pp. 307-347.

4. Adelman, H. M., et al, "An Isoparametric Quadrilateral Membrane Element for NASTRAN", in NASTRAN: Users' Experiences, NASA TM X-2639, Sept. 1972, pp. 315-336.

5. Everstine, G. C., "The BANDIT Computer Program for the Reduction of Matrix Bandwidth for NASTRAN", Naval Ship Research and Development Center, Report 3827, March 1972.

6. Joseph, G. A., MSC/NASTRAN Applications Manual, The MacNeal-Schwendler Corporation, November 1972.

7. McCormick, C. W., The NASTRAN Users' Manual, NASA SP-222(01), June 1972.

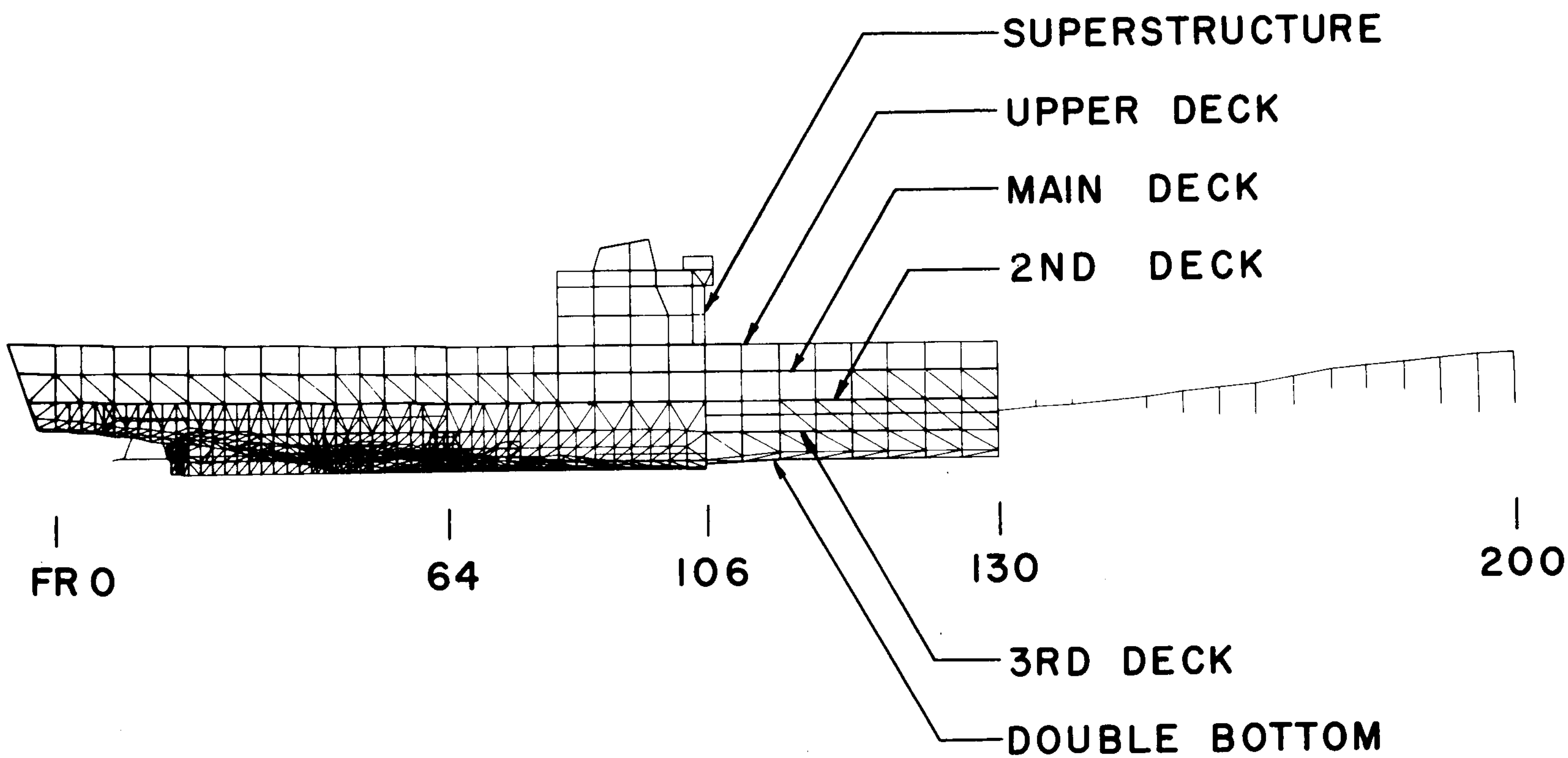

FIGURE 1. ELEVATION VIEW OF MODEL

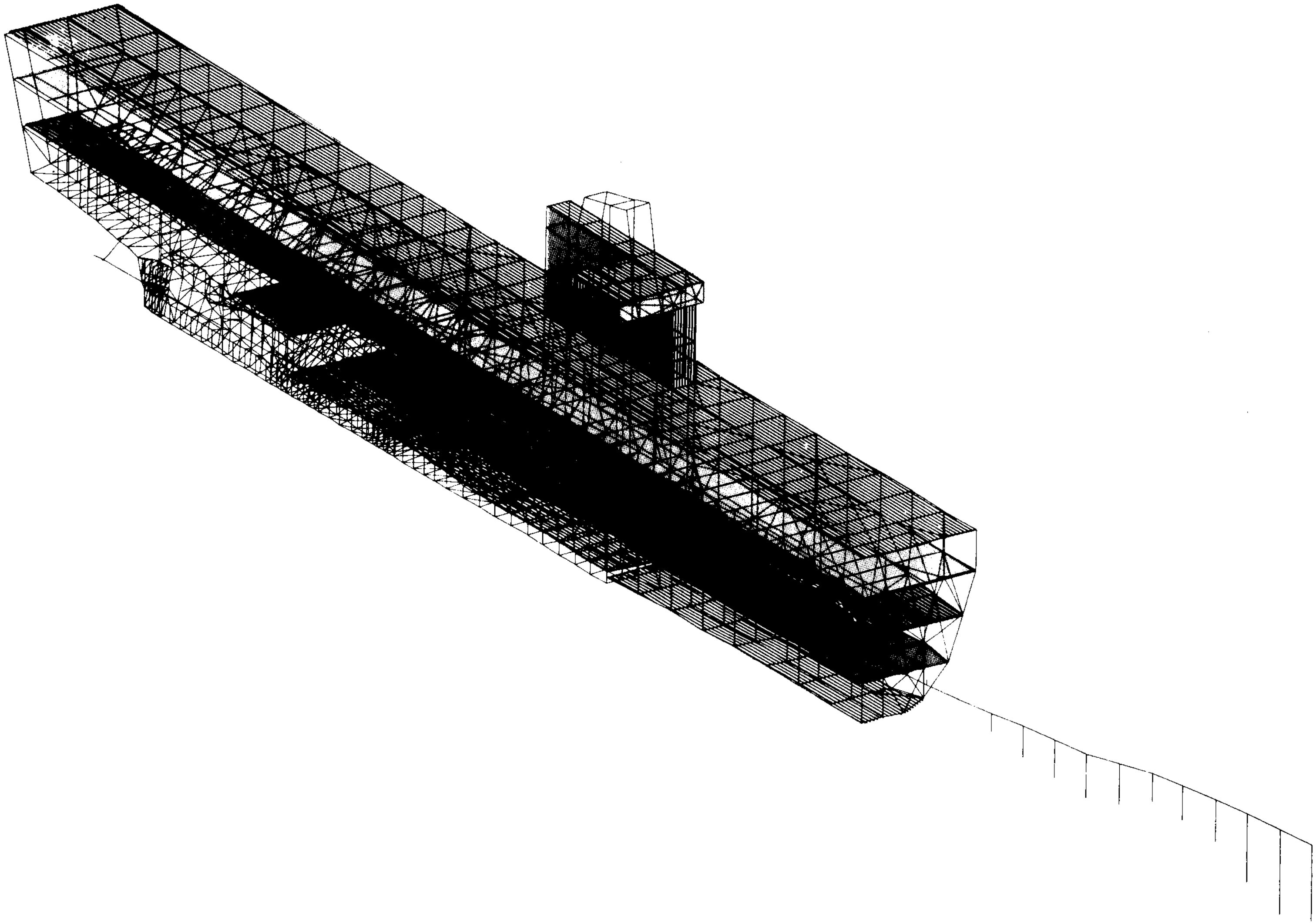

FIGURE 2. ROTATED VIEW OF MODEL—DECKS AND SUPERSTRUCTURE

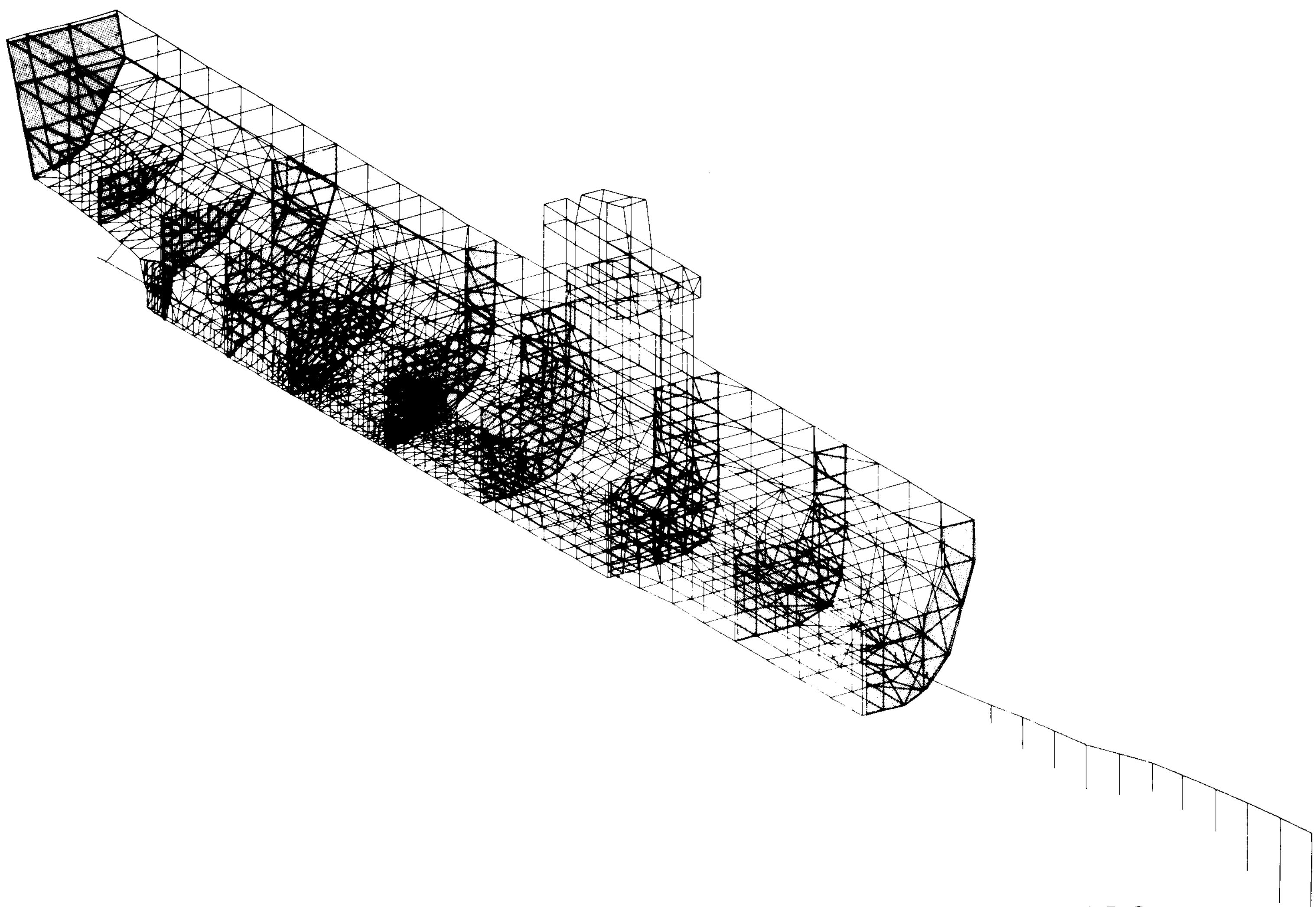

FIGURE 3. ROTATED VIEW OF MODEL — BULKHEADS

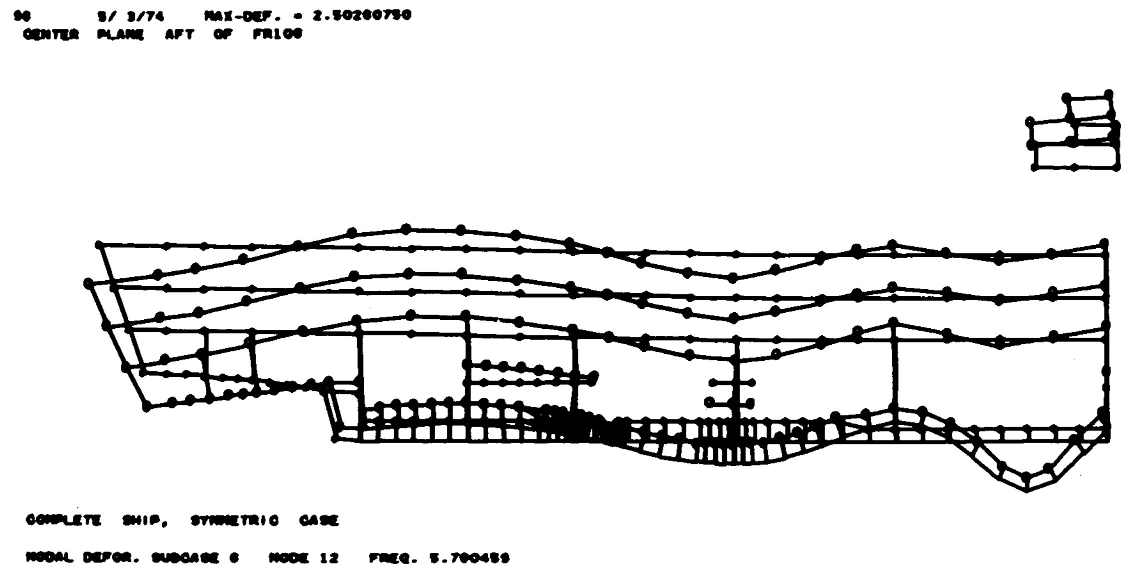

FIGURE 4. AFTERBODY ELEVATION ON CENTER LINE, SYMMETRIC MODE 12, 5.76 HZ.

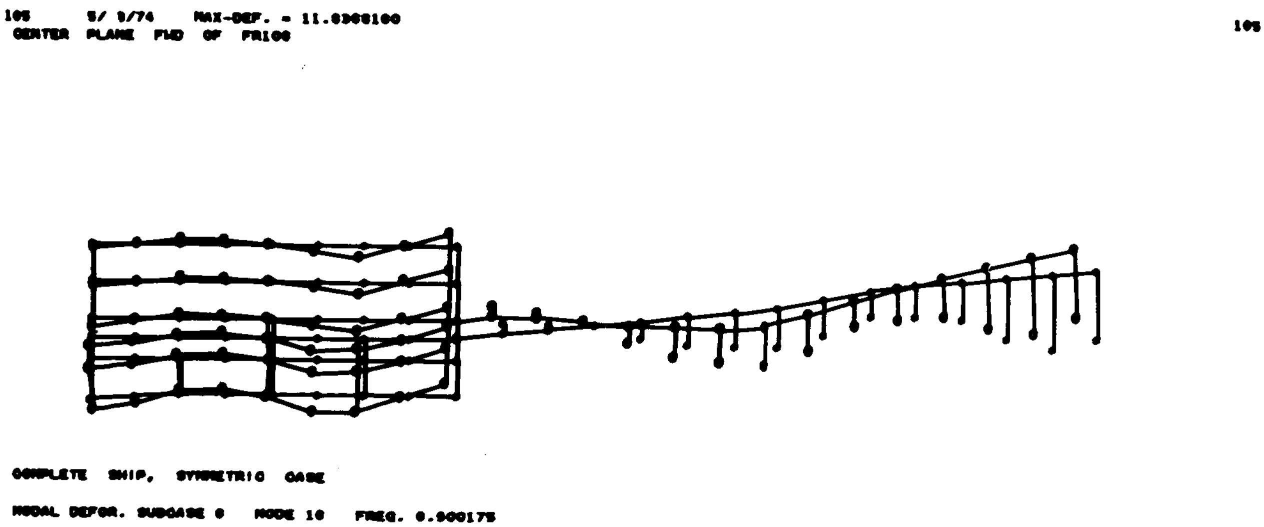

FIGURE 5. FOREBODY ELEVATION ON CENTER LINE, SYMMETRIC MODE 16, 6.90 HZ.

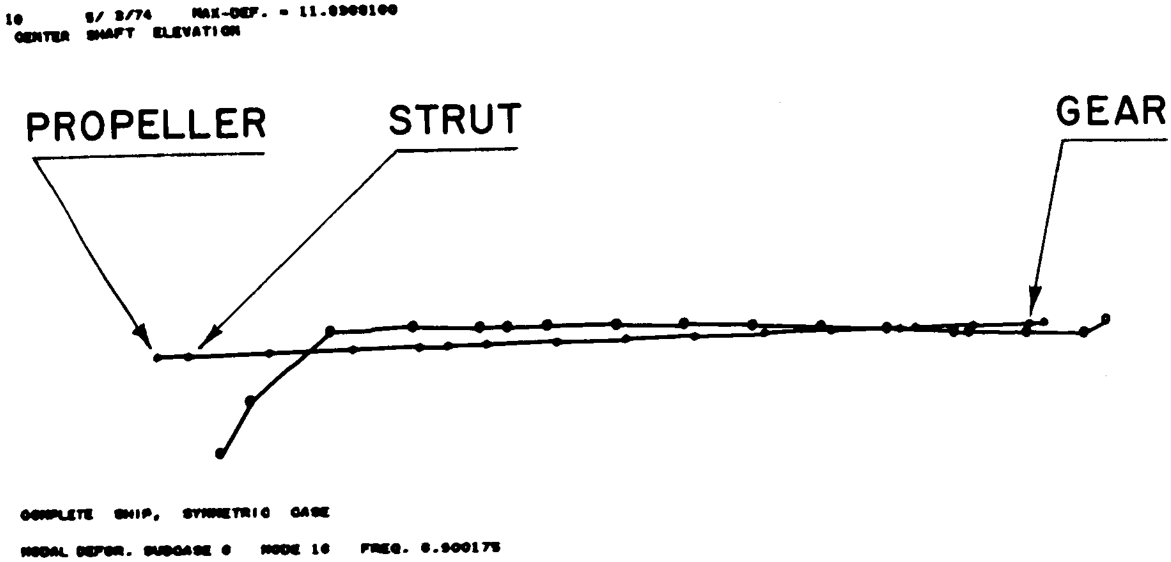

FIGURE 6. CENTER SHAFT ELEVATION, SYMMETRIC MODE 16, 6.90 HZ.

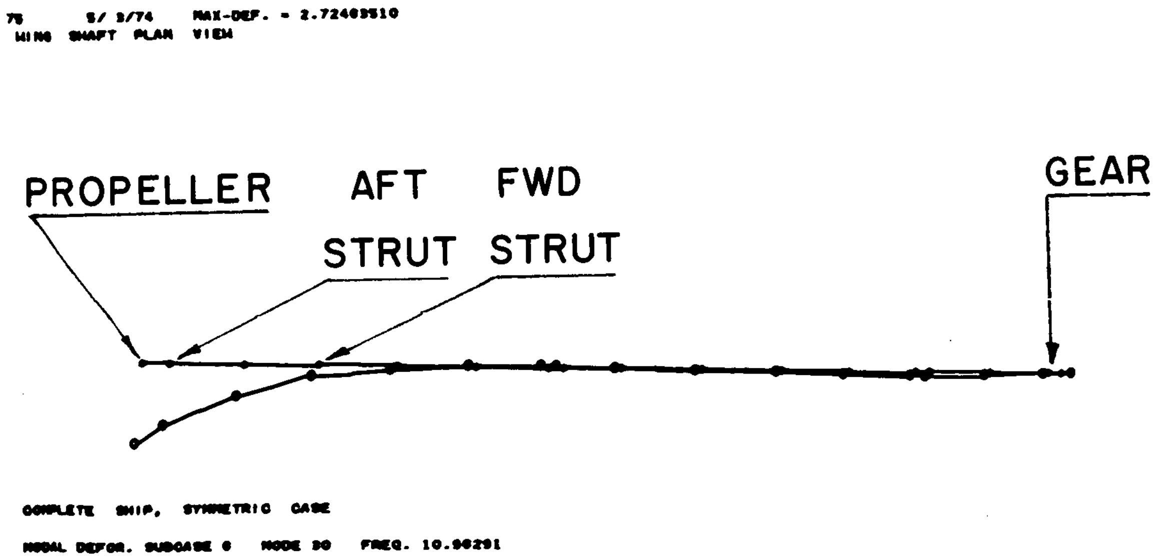

FIGURE 7. WING SHAFT PLAN VIEW, SYMMETRIC MODE 30, 10.96 HZ.

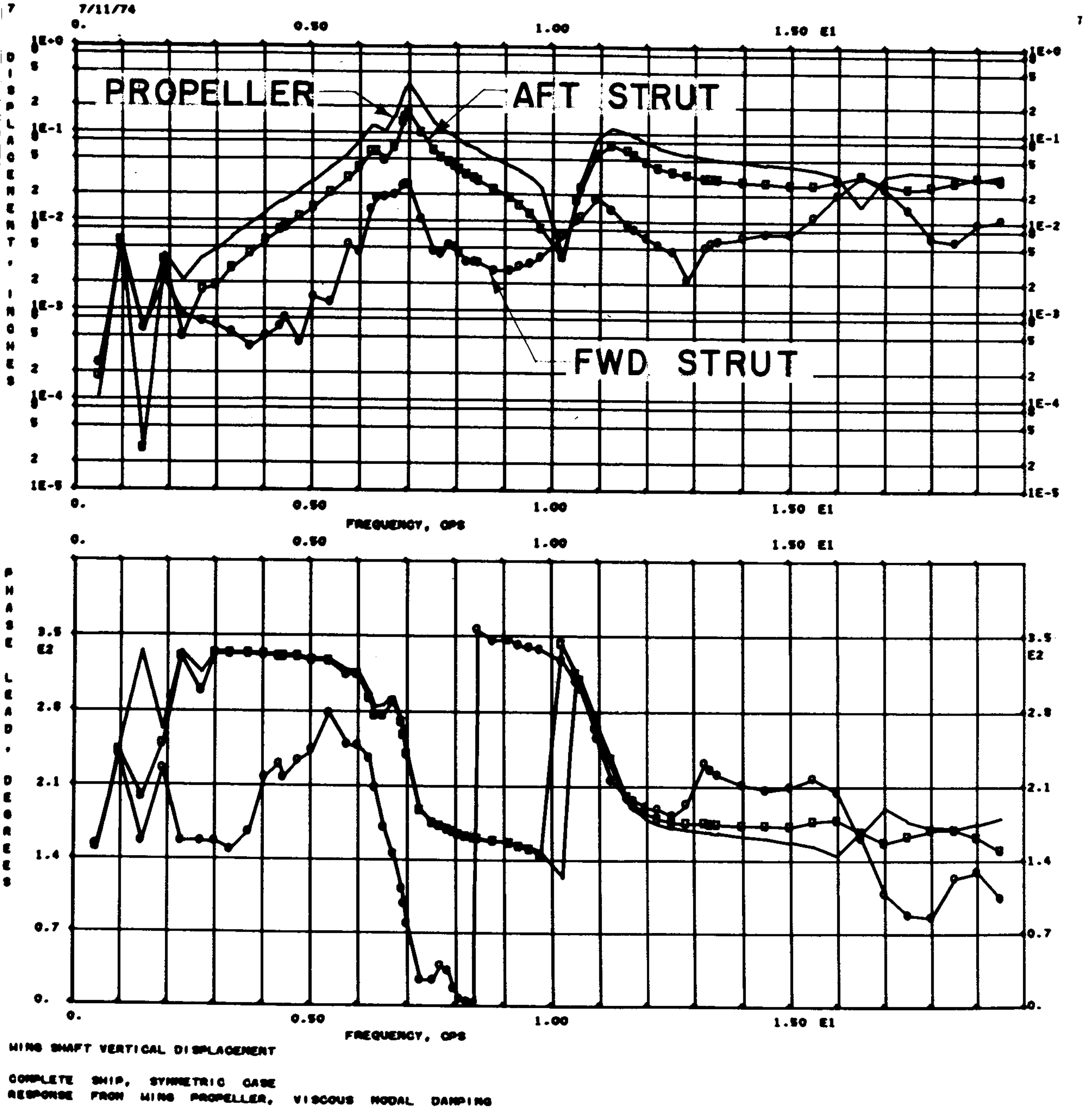

FIGURE 8. SYMMETRIC RESPONSE OF WING SHAFT TO WING PROPELLER EXCITATION.